Θ-PSO Algorithm for UPFC Based Output Feedback Damping Controller

Amin Safari

Department of Electrical Engineering,
Ahar Branch, Islamic Azad University, Ahar, Iran
a-safari@iau-ahar.ac.ir

Abstract

A novel approach based θ-Particle Swarm Optimization (θ-PSO) is proposed for optimal selection of the output feedback damping controller parameters for unified power flow controller (UPFC) in order to improve the damping of power system oscillations. The selection of the output feedback gains for the damping controllers is converted to an optimization problem with the time domain-based objective function which is solved by the θ-PSO algorithm. For designing, only local and available state variables are selected as the input stabilizing signals of each controller. Thus, structure of the proposed output feedback controller is simple and easy to implement. To ensure the robustness of the designed controllers, the design process takes into account a wide range of operating conditions and system configurations. Simulation results demonstrate that UPFC with the proposed output feedback controller can more effectively improve the dynamic stability, damp the oscillations, and enhance the transient stability of power system compared to the classical PSO and phase compensation based damping controllers. Moreover, the system performance analysis under different operating conditions shows that the δ_E based controller is superior to the m_B based controller.

Keywords: *Low Frequency Oscillations, Optimization, Output Feedback Damping Controller, UPFC, θ-PSO*

1. Introduction

The unified power flow controller (UPFC) is regarded as one of the most versatile devices in the flexible AC transmission systems (FACTS) device family [1-3]. It has the ability to control of the power flow in the transmission line, improve the transient stability, mitigate system oscillation and provide voltage support. It performs this through the control of the in-phase voltage, quadrate voltage and shunts compensation due to its mains control strategy [1, 4]. When the UPFC is applied to the interconnected power systems, it can also provide significant damping effect on tie-line power oscillation through its supplementary control.

Mathematical modeling and analysis of UPFC is presented in [5]. It presents an establishment of the linearized Phillips-Heffron model of a power system installed with a UPFC device. Some authors suggested different control schemes for a UPFC damping controller design such as fuzzy control, robust control and neural network [6-10]. However, the parameters adjustments of these controllers need some trial and error procedure. In general, for the simplicity of practical implementation of the controllers, decentralized output feedback control [11-13] with feedback signals available at the location of the each controlled device is most favorable. A new approach for the optimal design of UPFC based output feedback damping controller is investigated in this paper. Here, the design problem is converted to a constraints optimization problem. A performance index is defined based on the

system dynamics after an impulse disturbance alternately occurs in synchronous machine. Then a performance index is organized for a wide range of operating conditions and used to form the objective function of the design problem.

Recently, PSO technique is used for UPFC based output feedback damping controller design [11]. The PSO is a novel population based meta-heuristic, which utilizes the swarm intelligence generated by the cooperation and competition between the particle in a population and has emerged as the useful tool for engineering optimization. Unlike the other heuristic techniques, it has a flexible and well-balanced mechanism to improve the global and local exploration abilities. This algorithm has also been found to be robust in solving problems featuring non-linearity, non-differentiability and high-dimensionality [14-17]. Recently, many researchers have studied the performance of the PSO algorithm and a variety of the PSO was proposed and applied to various types of the engineering problems such as controller design [18-20]. From these studies, it can be concluded that the performance of the classical PSO greatly depends on its parameters, and by increasing the number of variables, the complexity of the search space increases dramatically and it often suffers the problem of being trapped in local optima point. In this paper a new strategy based PSO algorithm called θ-PSO [21] which is based on phase angle vector but not the velocity vector, is firstly applied for design of the UPFC damping controller in power systems. In θ-PSO, an increment of phase angle vector replaces velocity vector and the positions are adjusted by the mapping of phase angles. The design problem is formulated as an optimization problem and the θ-PSO is used to solve it. An effective damping controller ought to be designed to be robust to the changes of operating conditions and to be able to operate in a nonlinear environment. Recently researches [11] focus have been to design robust FACTS based damping controllers and some useful results have been published that consider the robustness of FACTS damping controllers to the variations of power-system operating conditions. The effectiveness of the proposed controller is demonstrated through nonlinear time simulation studies and some performance indices to damp low frequency oscillations under different operating conditions in comparison with the CPSO and phase compensation based damping controllers. Results evaluation show that the proposed method achieves good robust performance for damping the low frequency oscillations under different operating conditions.

2. Review of the CPSO and θ-PSO Techniques

2.1 CPSO

The PSO is a population-based algorithm and is described by its developers as an optimization paradigm, which models the social behavior of the birds flocking or fish schooling for food. Therefore, the PSO works with a population of potential solutions rather than with a single individual [14]. The PSO has also been found to be robust in solving problem featuring non-linearity, non-differentiability and high-dimensionality [17]. In the PSO technique a number of simple entities and the particles are placed in the search space of some problem or function and each evaluates the objective function at its current location. Then, each particle determines its movement through the search space by combining some aspect of the history of its own current and best locations by those of other members of the swarm with some random perturbations. The next iteration takes place after all particles have been moved. Eventually the swarm as a whole, like a flock of birds collectively foraging for food, is likely to move close to an optimum of the fitness function [16].

In the PSO technique, the trajectory of each individual in the search space is adjusted by dynamically altering the velocity of each particle, according to its own flying experience and the flying experience of the other particles in the search space. The position and the velocity vectors of the *i*th particle in the *D*-dimensional search space can be represented as $x_i = (x_{i1}, x_{i2}, \ldots, x_{iD})$ and $v_i = (v_{i1}, v_{i2} \ldots v_{iD})$ respectively. According to fitness function, let us say the best position of each particle, which corresponds to the best fitness value (*pbest*) obtained by that particle at time, be $P_i = (p_{i1}, p_{i2}, \ldots, p_{iD})$, and the global version of the PSO keeps track of the overall best value (*gbest*), and its location, obtained thus far by any particle in the population. Then, the new velocities and the positions of the particles for the next fitness evaluation are calculated using the following two equations [17, 18].

$$v_{id} = w \times v_{id} + c_1 \times r_1 \times (P_{id} - x_{id}) + c_2 \times r_2 \times (P_{gd} - x_{id}) \quad (1)$$

$$x_{id} = x_{id} + v_{id} \quad (2)$$

Where, P_{id} and P_{gd} are *pbest* and *gbest*. The positive constants c_1 and c_2 are the cognitive and social components that are the acceleration constants responsible for varying the particle velocity towards *pbest* and *gbest*, respectively. Variable r_1 and r_2 are a random functions based on uniform probability distribution functions in the range [0, 1]. The inertia weight *w* is responsible for dynamically adjusting the velocity of the particles, so it is responsible for balancing between local and global searches and hence requiring less iteration for the algorithm to converge. The following inertia weight is used in Eq. (1):

$$w = w_{\max} - \frac{w_{\max} - w_{\min}}{iter\_\max} iteration \quad (3)$$

Where, *iter_max* is the maximum number of iterations and *iteration* is the current number of iteration. The Equation (3) presents how the inertia weight is updated, considering w_{max} and w_{min} are the initial and final inertia weights, respectively.

2.2 θ-PSO

The θ-PSO algorithm is newly introduced strategy of PSO which is a simple algorithm, easy to implement. It is based on phase angle vector instead of the velocity vector and an increment of phase angle $\Delta\theta_i$ vector replaces velocity vector v_i. It is dynamically adjusted according to the historical behaviors of the particle and its companions. In the θ-PSO, the positions are adjusted by the mapping of phase angles, thus, a particle is represented by its phase angle θ and increment of phase angle $\Delta\theta$ and its position decided by a mapping function [21]. By considering the mentioned differences equations (1) and (2) are modified and the particles move according to the following iterative equations. The θ-PSO can be described with the following equations.

$$\Delta\theta_{id}(t+1) = w \times \Delta\theta_{id}(t) + c_1 r_1 (\theta p_{id} - \theta_{id}(t)) + c_2 r_2 (\theta g_{gd} - \theta_{id}(t)) \quad (4)$$

$$\theta_{id}(t+1) = \theta_{id}(t) + \Delta\theta_{id}(t+1) \quad (5)$$

$$x_{id}(t) = f(\theta_{id}(t)) \quad (6)$$

$$F'_i(t) = fitness value(x_i(t)) \quad (7)$$

With $\theta_{id} \in (\theta_{\min}, \theta_{\max}), \Delta\theta_{id} \in (\Delta\theta_{\min}, \Delta\theta_{\max}), x_{id} \in (x_{\min}, x_{\max})$ and f is being a monotonic mapping function. In this paper,

$$\theta_{id} \in (-\pi/2, \pi/2), \Delta\theta_{id} \in (-\pi/2, \pi/2)$$

$$f(\theta_{id}) = \frac{x_{\max} - x_{\min}}{2} \sin\theta_{id} + \frac{x_{\max} + x_{\min}}{2} \tag{8}$$

Where $d=1, 2, ..., D; i= 1, 2, ..., S$; the D, S, c_1, c_2, w, r_1, r_2 and $x_i(t)$ are the same as those in equations (1) and (2). The $\theta_i(t)$ is the phase angle of particle ith at time t; the $\Delta\theta_i(t)$ is the increment of particle i^{th} phase angle at time t; $\theta p_i(t)$ is the phase angle of the personal best solution of particle i^{th} at time t; $\theta g_g(t)$ is the phase angle of global best solution at time t; $F'_i(t)$ is the fitness value of particle i^{th} at time t which is identified by the function fitness value. The procedure of the θ-PSO can be summarized as following:

Initialize *a population with random phase angle* $\theta_i(t)$ *and the increment of the phase angle* $\Delta\theta_i(t)$*;*
Repeat $t=1, 2, ..., t_{max}$ *;*
For *each particle* $i=1, 2, ..., S$
If $t=1$
Calculate $x_i(1)$ *using Eq. (6);*
Calculate *the fitness value* $F'_i(1)$ *using Eq. (7);*
$F'_{pi}(1)= F'_i(1)$; $\theta_{pi}(1)= \theta_i(1)$;
$F'_g(1)= F'_i(1)$; $\theta_g(1)= \theta_i(1)$;
Else
Update *the increment of the phase angle* $\Delta\theta_i(t)$ *using Eq.(11) and limit* $\Delta\theta_i(t)$ *to* $(\Delta\theta_{min}(t), \Delta\theta_{max}(t))$*;*
Update $\theta_i(t)$ *using Eq. (5) and limit* $\theta_i(t)$ *to* $(\theta_{min}(t), \theta_{max}(t))$*;*
Update $x_i(t)$ *using Eq. (6);*
Update *the fitness value* $F'_i(t)$ *using Eq. (7);*
If $F'_i(t) < F'_{pi}(t)$
$F'_{pi}(t)=F'_i(t)$; $\theta_{pi}(1)= \theta_i(1)$;
End
If $F'_i(t) < F'_g(t)$
$F'_g(t)= F'_i(t)$; $\theta_g(t)= \theta_i(t)$;
End
End
End
Until *the stopping criterion is met;*

The $F'_{pi}(t)$ is the personal best fitness value of particle i^{th} at time t and $F'_g(t)$ is the global best fitness value at time t.

3. Power System Modeling With UPFC

Figure 1 shows a single machine infinite bus (SMIB) system equipped with a UPFC, which consists of an excitation transformer (ET), a boosting transformer (BT), two three-phase GTO based voltage source converters (VSCs), and a DC link capacitors. The four input control signals to the UPFC are m_E, m_B, δ_E, and δ_B, where, m_E is the excitation amplitude modulation ratio, m_B is the boosting amplitude modulation ratio, δ_E is the excitation phase

angle and δ_B is the boosting phase angle [18]. The system data is given in the Appendix. The main objective of the UPFC is to control the power flow in steady state conditions. However, high speed of operation of thyristor based devices makes it possible to also use UPFC dynamically to improve damping of power oscillations.

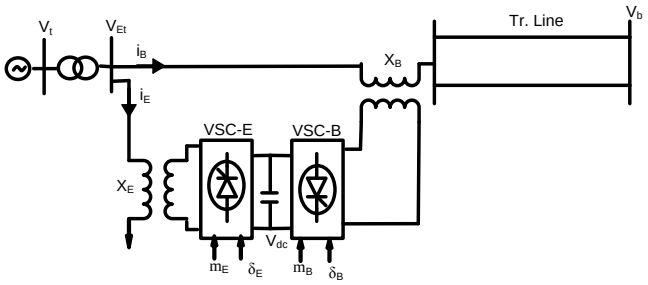

Figure 1. SMIB Power System Equipped with UPFC

3.1 Power System Nonlinear Model with UPFC

The dynamic model of the UPFC is required in order to study the effect of the UPFC for enhancing the small signal stability of the power system. By applying Park's transformation and neglecting the resistance and transients of the ET and BT transformers, the UPFC can be modeled as [5]:

$$\begin{bmatrix} v_{Etd} \\ v_{Etq} \end{bmatrix} = \begin{bmatrix} 0 & -x_E \\ x_E & 0 \end{bmatrix} \begin{bmatrix} i_{Ed} \\ i_{Eq} \end{bmatrix} + \begin{bmatrix} \frac{m_E \cos\delta_E v_{dc}}{2} \\ \frac{m_E \sin\delta_E v_{dc}}{2} \end{bmatrix} \tag{9}$$

$$\begin{bmatrix} v_{Btd} \\ v_{Btq} \end{bmatrix} = \begin{bmatrix} 0 & -x_B \\ x_B & 0 \end{bmatrix} \begin{bmatrix} i_{Bd} \\ i_{Bq} \end{bmatrix} + \begin{bmatrix} \frac{m_B \cos\delta_B v_{dc}}{2} \\ \frac{m_B \sin\delta_B v_{dc}}{2} \end{bmatrix} \tag{10}$$

$$\dot{v}_{dc} = \frac{3m_E}{4C_{dc}} [\cos\delta_E \quad \sin\delta_E] \begin{bmatrix} i_{Ed} \\ i_{Eq} \end{bmatrix} + \frac{3m_B}{4C_{dc}} [\cos\delta_B \quad \sin\delta_B] \begin{bmatrix} i_{Bd} \\ i_{Bq} \end{bmatrix} \tag{11}$$

Where, v_{Et}, i_E, v_{Bt}, and i_B are the excitation voltage, excitation current, boosting voltage, and boosting current, respectively; C_{dc} and v_{dc} are the DC link capacitance and voltage. The nonlinear model of the SMIB system is described by [1]:

$$\dot{\delta} = \omega_0 (\omega - 1) \tag{12}$$

$$\dot{\omega} = (P_m - P_e - D\Delta\omega)/M \tag{13}$$

$$\dot{E}'_q = (-E_q + E_{fd})/T'_{do} \tag{14}$$

$$\dot{E}_{fd} = (-E_{fd} + K_a(V_{ref} - V_t))/T_a \tag{15}$$

Where, where δ is the rotor angle, ω the rotor speed, P_m the mechanical input power, P_e the electrical output power, E'_q the internal voltage behind x'$_d$, E_{fd} the equivalent excitation voltage, T_e the electric torque, T'_{do} the time constant of excitation circuit, K_A the regulator gain, T_A the regulator time constant, v_{ref} the reference voltage and v is the terminal voltage.

$$P_e = V_{td} I_{td} + V_{tq} I_{tq}; E_q = E'_{qe} + (X_d - X'_d) I_{td}; V_t = V_{td} + jV_{tq};$$
$$V_{td} = X_q I_{tq}; V_{tq} = E'_q - X'_d I_{td}; I_{td} = I_{tld} + I_{Ed} + I_{Bd}; I_{tq} = I_{tlq} + I_{Eq} + I_{Bq}$$

From Figure 1, we can have:

$$\bar{v}_t = jx_{tE}(\bar{i}_B + \bar{i}_E) + \bar{v}_{Et} \tag{16}$$

$$\bar{v}_{Et} = \bar{v}_{Bt} + jx_{BV}\bar{i}_B + \bar{v}_b \tag{17}$$

Where, i_t and v_b, are the armature current and infinite bus voltage, respectively. From the above equations, we can obtain:

$$i_{Ed} = \frac{x_{BB}}{x_{d\Sigma}} E'_q - \frac{m_E \sin\delta_E v_{dc} x_{Bd}}{2x_{d\Sigma}} + \frac{x_{dE}}{x_{d\Sigma}}(v_b \cos\delta + \frac{m_B \sin\delta_B v_{dc}}{2}) \tag{18}$$

$$i_{Eq} = \frac{m_E \cos\delta_E v_{dc} x_{Bq}}{2x_{q\Sigma}} - \frac{x_{qE}}{x_{q\Sigma}}(v_b \sin\delta + \frac{m_B \cos\delta_B v_{dc}}{2}) \tag{19}$$

$$i_{Bd} = \frac{x_E}{x_{d\Sigma}} E'_q + \frac{m_E \sin\delta_E v_{dc} x_{dE}}{2x_{d\Sigma}} - \frac{x_{dt}}{x_{d\Sigma}}(v_b \cos\delta + \frac{m_B \sin\delta_B v_{dc}}{2}) \tag{20}$$

$$i_{Bq} = -\frac{m_E \cos\delta_E v_{dc} x_{qE}}{2x_{q\Sigma}} + \frac{x_{qt}}{x_{q\Sigma}}(v_b \sin\delta + \frac{m_B \cos\delta_B v_{dc}}{2}) \tag{21}$$

Where, x_E , x_B , x_d , x'_d and x_q are the ET , BT reactance, d-axis reactance, d-axis transient reactance, and q-axis reactance, respectively.

3.2 Power System Linearized Model

A linear dynamic model is obtained by linearizing the nonlinear model round an operating condition. The linearized model of power system is given as follows:

$$\Delta\dot{\delta} = \omega_0 \Delta\omega \tag{22}$$

$$\Delta\dot{\omega} = (-\Delta P_e - D\Delta\omega)/M \tag{23}$$

$$\Delta\dot{E}'_q = (-\Delta E_q + \Delta E_{fd})/T'_{do} \tag{24}$$

$$\Delta\dot{E}_{fd} = (K_A(\Delta v_{ref} - \Delta v) - \Delta E_{fd})/T_A \tag{25}$$

$$\Delta\dot{v}_{dc} = K_7\Delta\delta + K_8\Delta E'_q - K_9\Delta v_{dc} + K_{ce}\Delta m_E + K_{c\delta e}\Delta\delta_E + K_{cb}\Delta m_B + K_{c\delta b}\Delta\delta_B \tag{26}$$

$$\Delta P_e = K_1\Delta\delta + K_2\Delta E'_q + K_{pd}\Delta v_{dc} + K_{pe}\Delta m_E + K_{p\delta e}\Delta\delta_E + K_{pb}\Delta m_B + K_{p\delta b}\Delta\delta_B \tag{27}$$

$$\Delta E'_q = K_4\Delta\delta + K_3\Delta E'_q + K_{qd}\Delta v_{dc} + K_{qe}\Delta m_E + K_{q\delta e}\Delta\delta_E + K_{qb}\Delta m_B + K_{q\delta b}\Delta\delta_B \tag{28}$$

$$\Delta V_t = K_5\Delta\delta + K_6\Delta E'_q + K_{vd}\Delta v_{dc} + K_{ve}\Delta m_E + K_{v\delta e}\Delta\delta_E + K_{vb}\Delta m_B + K_{v\delta b}\Delta\delta_B \tag{29}$$

Where, K_1, $K_2 \ldots K_9$, K_{pu} ,K_{qu} and K_{vu} are linearization constants. The state-space model of power system is given by:

$$\dot{x} = Ax + Bu \tag{30}$$

Where, the state vector x, control vector u, A and B are:

$$x=[\Delta\delta \quad \Delta\omega \quad \Delta E'_q \quad \Delta E_{fd} \quad \Delta v_{dc}] \;;\; u=[\Delta m_E \quad \Delta\delta_E \quad \Delta m_B \quad \Delta\delta_B]^T$$

$$A=\begin{bmatrix} 0 & w_0 & 0 & 0 & 0 \\ -\frac{K_1}{M} & 0 & -\frac{K_2}{M} & 0 & -\frac{K_{pd}}{M} \\ -\frac{K_4}{T'_{do}} & 0 & -\frac{K_3}{T'_{do}} & \frac{1}{T'_{do}} & -\frac{K_{qd}}{T'_{do}} \\ -\frac{K_A K_5}{T_A} & 0 & -\frac{K_A K_6}{T_A} & -\frac{1}{T_A} & -\frac{K_A K_{vd}}{T_A} \\ K_7 & 0 & K_8 & 0 & -K_9 \end{bmatrix} ; \quad B=\begin{bmatrix} 0 & 0 & 0 & 0 \\ -\frac{K_{pe}}{M} & -\frac{K_{p\delta e}}{M} & -\frac{K_{pb}}{M} & -\frac{K_{p\delta b}}{M} \\ -\frac{K_{qe}}{T'_{do}} & -\frac{K_{q\delta e}}{T'_{do}} & -\frac{K_{qb}}{T'_{do}} & -\frac{K_{q\delta b}}{T'_{do}} \\ -\frac{K_A K_{vc}}{T_A} & -\frac{K_A K_{v\delta e}}{T_A} & -\frac{K_A K_{vb}}{T_A} & -\frac{K_A K_{v\delta b}}{T_A} \\ K_{ce} & K_{c\delta e} & K_{cb} & K_{c\delta b} \end{bmatrix} \tag{31}$$

3.3 Output Feedback Controller Design using θ-PSO

A power system can be described by a linear time invariant (LTI) state space model as follows [12]:

$$\begin{aligned} \dot{x} &= Ax + Bu \\ y &= Cx \end{aligned} \tag{32}$$

Where x, y and u denote the system linearized state, output and input variable vectors, respectively. A, B and C are constant matrixes with appropriate dimensions which are dependent on the operating point of the system. The eigenvalues of the state matrix A that are called the system modes define the stability of the system when it is affected by a small interruption. As long as all eigenvalues have negative real parts, the power system is stable when it is subjected to a small disturbance. If one of these modes has a positive real part the system is unstable. In this case, using either the output or the state feedback controller can move the unstable mode to the left-hand side of the complex plane in the area of the negative real parts. An output feedback controller has the following structures [11]:

$$u = -Gy \tag{33}$$

Substituting (33) into (32) the resulting state equation is:

$$\dot{x} = A_C x \tag{34}$$

Where, A_c is the closed-loop state matrix and is given by:

$$A_C = A - BGC \tag{35}$$

By properly choosing the feedback gain G, the eigenvalues of closed-loop matrix A_c are moved to the left-hand side of the complex plane and the desired performance of controller can be achieved. The output feedback signals can be selected by using mode observability analysis [12]. Once the output feedback signals are selected, only the selected signals are used in forming equation (32). Thus, the remaining problem in the design of output feedback

controller is the selection of G to achieve the required objectives. The control objective is to increase the damping of the critical modes to the desired level. In this paper, δ_E and m_B are modulated in order to output feedback damping controller design and are compared with the classical PSO based controller. The proposed controller must be able to work well under all the operating conditions where the improvement in damping of the critical modes is necessary. This work employs the θ-PSO [21] to improve optimization synthesis and find the global optimum value of objective function. In this study, an Integral of Time multiplied Absolute value of the Error (ITAE) is taken as the objective function. Since the operating conditions in power systems are often varied, a performance index for a wide range of operating points is defined as follows:

$$J = \sum_{i=1}^{Np} \int_{0}^{tsim} t|\Delta\omega_i|dt \tag{36}$$

Where, t_{sim} is the time range of simulation and N_P is the total number of operating points for which the optimization is carried out. For objective function calculation, the time-domain simulation of the power system model is carried out for the simulation period. It is aimed to minimize this objective function in order to improve the system response in terms of the settling time and overshoots. The design problem can be formulated as the following constrained optimization problem, where the constraints are the controller parameters bounds:

Minimize J Subject to*:*

$$\begin{aligned} G_1^{\min} \le G_1 \le G_1^{\max} \\ G_2^{\min} \le G_2 \le G_2^{\max} \end{aligned} \tag{37}$$

Typical ranges of the optimized parameters are [0.01-150] for G_1 and [0.01-10] for G_2. The flowchart of the output feedback controller design is depicted in Figure 2.

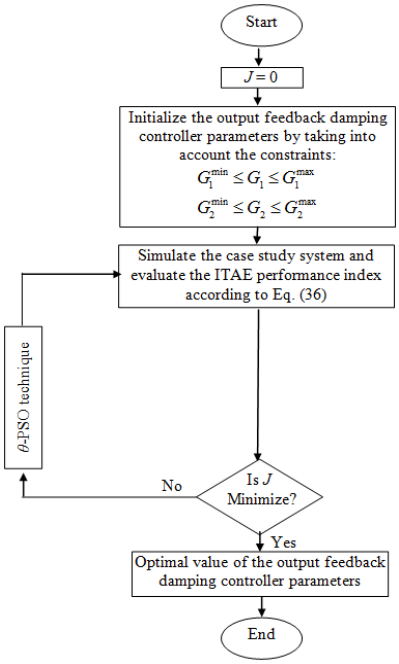

Figure 2. Flowchart of the Output Feedback Controller Design

The optimization of UPFC controller parameters is carried out by evaluating the fitness function as given in Eq. (36), which considers a multiple of operating conditions. The operating conditions are considered as:

- Base case: P = 0.80pu, Q = 0.114 pu and X_L=0.3 pu.
- Case 1: P = 0.2 pu, Q = 0.01 and X_L=0.3 pu.
- Case 2: P = 1.20 pu, Q = 0.4 and X_L=0.3 pu.
- Case 3: P = 0.80pu, Q = 0.114 pu and X_L=0.6 pu.
- Case 4: P = 1.20 pu, Q = 0.4 and X_L=0.6 pu.

In order to acquire better performance the input parameters that control the θ-PSO, *i.e.*, number of particle, dimension size (D), the number of iteration, c_1 and c_2 is chosen as 30, 5, 60, 1.7 and 1.7, respectively. The final values of the optimized parameters are given in Table 1.

Table 1. The Optimal Parameter Settings of the Output Feedback Controllers

Controller	θ-PSO		CPSO	
	G_1	G_2	G_1	G_2
m_B	135.76	4.221	115.14	3.127
δ_E	81.30	0.607	60.18	0.31

4. Nonlinear Time-Domain Simulation

To assess the effectiveness and robustness of the designed controller based proposed algorithm, simulation studies are carried out for various fault disturbances and fault clearing sequences for two scenarios.

4.1 Scenario 1

In this scenario, the performance of the designed controller under transient conditions is verified by applying a 6-cycle three-phase fault at t = 1 sec, at the middle of the one transmission line. The fault is cleared by permanent tripping of the faulted line. The speed deviation of generator at three loading conditions due to designed controller based on the m_B and δ_E are shown in Figures 3 and 4. The response with the proposed robust controller can be observed to be much superior in comparison with the CPSO based output feedback controller.

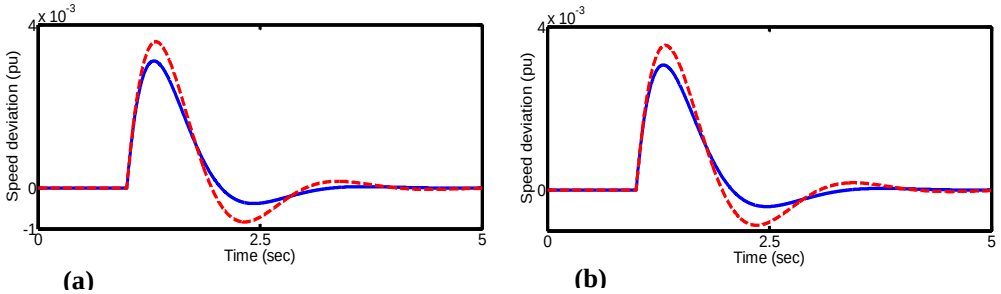

Figure 3. Dynamic Responses for Δω in Scenario 1 with δ_E based Controller at (a) base case (b) case 2 loading; Solid (θ-PSO) and Dashed (CPSO [11])

4.2 Scenario 2

In this scenario, another severe disturbance is considered for different loading conditions; that is, a 6-cycle, three-phase fault is applied at the same above mentioned location in scenario 1. The fault is cleared without line tripping and the original system is restored upon the clearance of the fault. The system response to this disturbance is shown in Figures 5 and 6. It is also clear from the figure that the θ-PSO based output feedback controller has good damping characteristics for low frequency oscillations and stabilizes the system quickly.

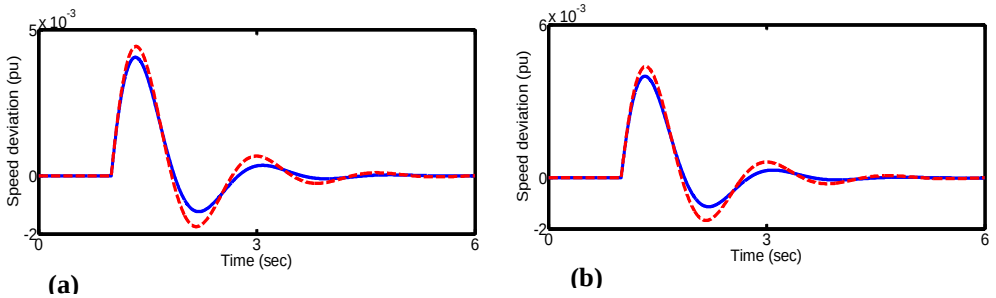

Figure 4. Dynamic Responses for Δω in Scenario 1 with m_B based Controller at (a) base case (b) case 2 loading; Solid (θ-PSO) and Dashed (CPSO [11])

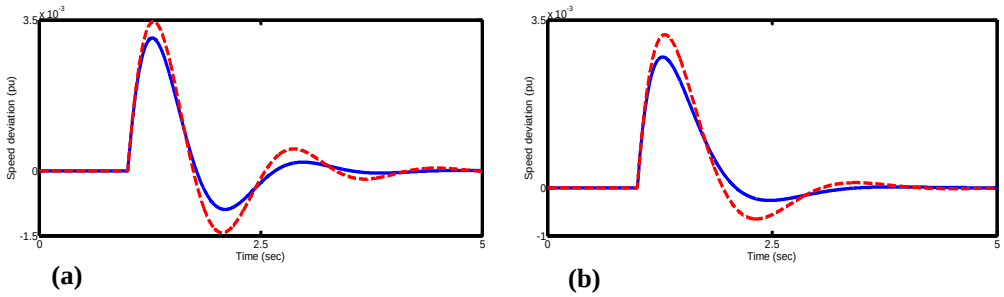

Figure 5. Dynamic Responses for Δω in Scenario 2 with δ_E based Controller at (a) base case (b) case 4 loading; Solid (θ-PSO) and Dashed (CPSO [11])

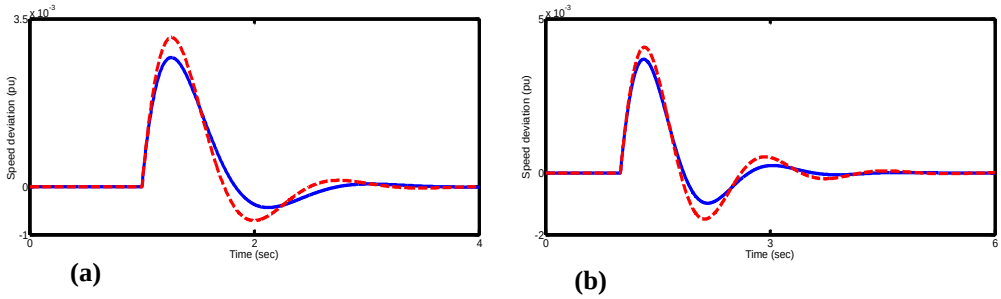

Figure 6. Dynamic Responses for Δω in Scenario 2 with m_B based Controller at (a) base case (b) case 4 loading; Solid (θ-PSO) and Dashed (CPSO [11])

From the above conducted tests, it can be concluded that the δ_E based controller is superior to the m_B based controller. To demonstrate robustness and performance of the proposed method, two performance indices: the ITAE and Figure of Demerit (FD) based on the system characteristics are defined as [11]:

$$ITAE = 10000\int_0^5 t|\Delta\omega|dt$$
$$FD = (1000\times OS)^2 + (4000\times US)^2 + T_s^2 \quad (38)$$

Where, speed deviation (Δω), Overshoot (OS), Undershoot (US) and settling time of speed deviation of the machine is considered for evaluation of the ITAE and FD indices. Numerical results of performance index ITAE for three loading cases are shown in Figures 7 and 8. The values of index FD with the disturbances considered are provided in Table 2.

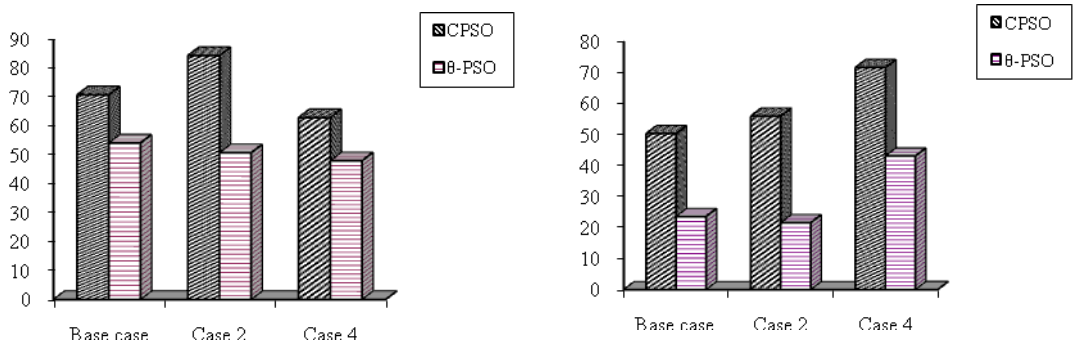

Figure 7. Values of the Performance Index ITAE with m_B Controller in a) scenario 1 and b) scenario 2

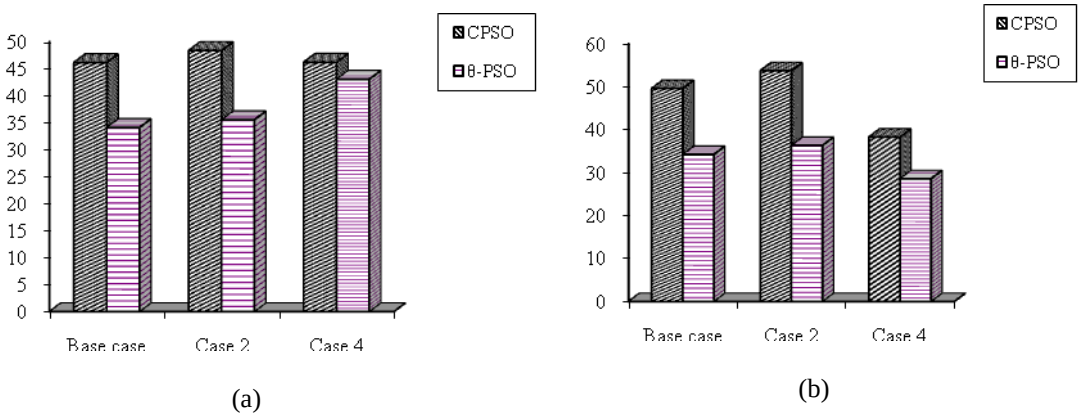

Figure 8. Values of the Performance Index ITAE with δ_E Controller in a) scenario 1 and b) scenario 2

It is worth mentioning that the lower the value of these indices is the better the system response in terms of time domain characteristics. It can be seen that the values of these system performance characteristics with the output feedback δ_E based

controller are much smaller compared to output feedback m_B based controller. This demonstrates that the overshoot, undershoot, settling time and speed deviations of the machine are greatly reduced by applying the proposed control approach.

Table 2. Values of Performance Index FD

Fault case	Controller	Base Case		Case 2		Case 4	
		θ-PSO	CPSO	θ-PSO	CPSO	θ-PSO	CPSO
Scenario 1	m_B	57.16	130.4	48.55	122.39	165.57	84.48
	δ_E	21.13	37.55	21.69	39.01	17	23.32
Scenario 2	m_B	17	63.01	15.51	70. 32	40.53	98.62
	δ_E	33.077	60.44	35.25	65.10	17.72	29.50

5. Conclusions

In this paper, the output feedback controller based the θ-PSO algorithm is successfully applied to design the UPFC to improve dynamic stability. The output feedback method can realize to stabilize the power system by using only the observable output so the implementation of the designed stabilizers becomes more feasible. The design problem of the robustly selecting output feedback controller parameters is converted into an optimization problem. The effectiveness of the proposed controller for improving transient stability performance of a power system are demonstrated by a weakly connected example power system subjected to different severe disturbances under different operating conditions. The computer simulation results show that the oscillations of synchronous machine can be quickly and effectively damped for case study system with the proposed controller. The system performance characteristics in terms of 'ITAE' and 'FD' indices show that the θ-PSO based output feedback damping controller demonstrates its superiority than the CPSO based output feedback controller at various fault disturbances and fault clearing sequences.

APPENDIX

The nominal parameters and operating condition of the system are listed in Tale 3.

Table 3. System Parameters

Generator	$M = 8$ MJ/MVA	$T'_{do} = 5.044$ s	$X_d = 1$pu
	$X_q = 0.6$p.u	$X'_d = 0.3$pu	$D = 0$
Excitation system		$K_a = 10$	$T_a = 0.05$s
Transformers		$X_T = 0.1pu$	$X_E = 0.1pu$
		$X_B = 0.1pu$	
DC link parameter		$V_{DC} = 2pu$	$C_{DC} = 1pu$
UPFC parameter		$m_B = 0.08$	$\delta_B = -78.21^\circ$
		$\delta_E = -85.35^\circ$	$m_E = 0.4$

References

[1] N. Tambey and M. Kothari, "Unified power flow controller based damping controllers for damping low frequency oscillations in a power system", IEE Proc. Gen, Transm, Distrib, vol. 150, no. 2, **(2003)**, pp. 129-140.

[2] L. Gyugyi, "Unified power-flow control concept for flexible ac transmission systems", IEE Proc. Gen. Transm, Distrib., vol. 139, no. 4, **(1992)**, pp. 323-331.

[3] N. G. Hingorani and L. Gyugyi, "Understanding FACTS: concepts and technology of flexible AC transmission systems", Wiley-IEEE Press**; (1999)**.

[4] Y. H. Song and A. T. Johns, "Flexible ac transmission systems (FACTS)", UK: IEE Press; **(1999)**.

[5] H. F. Wang, "A unified model for the analysis of FACTS devices in damping power system oscillations - Part III: unified power flow controller", IEEE Trans Power Deliv., vol. 15, no. 3, **(2000)**, pp. 978-983.

[6] A. Kazemi and M. Vakili Sohrforouzani, "Power system damping controlled facts devices", Elect. Power Energy Syst., vol. 28, **(2006)**, pp. 349-357.

[7] M. Vilathgamuwa, X. Zhu and S. S. Choi, "A robust control method to improve the performance of a unified power flow controller", Elect. Power Syst. Res., vol. 55, **(2000)**, pp. 103-111.

[8] P. K. Dash, S. Mishra and G. Panda, "A radial basis function neural network controller for UPFC", IEEE Trans. Power Syst., vol. 15, no. 4, **(2000)**, pp. 1293-1299.

[9] B. C. Pal, "Robust damping of interarea oscillations with unified power flow controller", IEE Proc. Gen. Transm. Distrib., vol. 149, no. 6, **(2002)**, pp. 733-738.

[10] P. K. Dash, S. Mishra and G. Panda, "Damping multimodal power system oscillation using hybrid fuzzy controller for series connected FACTS devices", IEEE Trans. Power Syst., vol. 15, no. 4, **(2000)**, pp. 1360-1366.

[11] H. Shayeghi, H. A. Shayanfar, S. Jalilzadeh and A. Safari, "Design of output feedback UPFC controllers for damping of electromechanical oscillations using PSO", Energy Convers Manage, vol. 50, **(2009)**, pp. 2554-2561.

[12] S. Lee, "Optimal decentralized design for output-feedback power system stabilizers", IEE Proc. Gener. Transm. Distrib., vol. 152, no. 4, **(2005)**, pp. 494-502.

[13] X. R. Chen, N. C. Pahalawaththa, U. D. Annakkage and C. S. Cumble, "Design of decentralized output feedback TCSC damping controllers by using simulated annealing", IEE Proc. Gen. Transm. Dist., vol. 145, no. 5, **(1998)**, pp. 553-558.

[14] J. Kennedy, R. Eberhart and Y. Shi, "Swarm intelligence", Morgan Kaufmann Publishers, San Francisco, **(2001)**.

[15] M. Clerc and J. Kennedy, "The particle swarm-explosion, stability, and convergence in a multidimensional complex space", IEEE Trans. Evol Comput, vol. 6, no. 1, **(2002)**, pp. 58-73.

[16] R. Poli, J. Kennedy and T. Blackwell, "Particle swarm optimization: An overview", Swarm Intelligent., vol. 1, **(2007)**, pp. 33-57.

[17] H. Shayeghi, A. Jalili and H. A. Shayanfar, "Multi-stage fuzzy load frequency control using PSO", Energy Conver. Manage., vol. 49, **(2008)**, pp. 2570-2580.

[18] H. Shayeghi, H. A. Shayanfar, S. Jalilzadeh and A. Safari, "A quantum particle swarm optimizer for the tuning of Unified Power Flow Controller", Energy Conver. Manage, vol. 51, **(2010)**, pp. 2299-2306.

[19] T. K. Das, G. K. Venayagamoorthy and U. O. Aliyu, "Bio-inspired algorithms for the design of multiple optimal power system stabilizers: SPPSO and BFA", IEEE Trans. Ind Appl, vol. 44, no. 5, **(2008)**, pp. 1445-1457.

[20] A. Safari, H. Shayeghi, "Iteration particle swarm optimization procedure for economic load dispatch with generator constraints", Exp Syst Appl, vol. 38, **(2011)**, pp. 6043-6048.

[21] W. Zhong, S. Li and F. Qian, "θ-PSO: a new strategy of particle swarm optimization", J. Zhejiang Univ. Sci., vol. 9, no. 6, **(2008)**, pp. 786-790.

Author

Amin Safari

He received the B.Sc. and M.Sc. degrees in Electrical Engineering in 2007 and 2009, respectively. Currently, he is a Ph.D. student of Power Electrical Engineering, Iran University of Science and Technology, Tehran, Iran. His areas of interest in research are Application of artificial intelligence to power system control design, FACTS device and fuzzy sets and systems. He has published more than 60 papers in international journals and conference proceedings. He joined to Islamic Azad University, Ahar branch, Iran, as lecture in 2009.